RYR1 and RYR3 Have Different Roles in the Assembly of Calcium Release Units of Skeletal Muscle

Feliciano Protasi,* Hiroaki Takekura,† Yaming Wang,* S. R. Wayne Chen,‡ Gerhard Meissner,§ Paul D. Allen,* and Clara Franzini-Armstrong†

*Department of Anesthesia Research, Brigham and Women's Hospital, Boston, Massachusetts 02115 USA; †Department of Cell and Developmental Biology, University of Pennsylvania, Philadelphia, Pennsylvania 19104 USA; ‡Department of Biochemistry and Molecular Biology, University of Calgary, Calgary, Alberta, Canada; and §Department of Biochemistry and Biophysics, University of North Carolina, Chapel Hill, North Carolina 27599 USA

ABSTRACT　Calcium release units (CRUs) are junctions between the sarcoplasmic reticulum (SR) and exterior membranes that mediates excitation contraction (e-c) coupling in muscle cells. In skeletal muscle CRUs contain two isoforms of the sarcoplasmic reticulum Ca^{2+} release channel: ryanodine receptors type 1 and type 3 (RyR1 and RyR3). 1B5s are a mouse skeletal muscle cell line that carries a null mutation for RyR1 and does not express either RyR1 or RyR3. These cells develop dyspedic SR/exterior membrane junctions (i.e., dyspedic calcium release units, dCRUs) that contain dihydropyridine receptors (DHPRs) and triadin, two essential components of CRUs, but no RyRs (or feet). Lack of RyRs in turn affects the disposition of DHPRs, which is normally dictated by a linkage to RyR subunits. In the dCRUs of 1B5 cells, DHPRs are neither grouped into tetrads nor aligned in two orthogonal directions. We have explored the structural role of RyR3 in the assembly of CRUs in 1B5 cells independently expressing either RyR1 or RyR3. Either isoform colocalizes with DHPRs and triadin at the cell periphery. Electron microscopy shows that expression of either isoform results in CRUs containing arrays of feet, indicating the ability of both isoforms to be targeted to dCRUs and to assemble in ordered arrays in the absence of the other. However, a significant difference between RyR1- and RyR3-rescued junctions is revealed by freeze fracture. While cells transfected with RyR1 show restoration of DHPR tetrads and DHPR orthogonal alignment indicative of a link to RyRs, those transfected with RyR3 do not. This indicates that RyR3 fails to link to DHPRs in a specific manner. This morphological evidence supports the hypothesis that activation of RyR3 in skeletal muscle cells must be indirect and provides the basis for failure of e-c coupling in muscle cells containing RyR3 but lacking RyR1 (see the accompanying report, Fessenden et al., 2000).

INTRODUCTION

Ryanodine receptors (RyRs) are large intracellular channels (~2260 kDa) that play an important role in Ca^{2+} signaling in a large variety of cells (for reviews see Coronado et al., 1994; Meissner, 1994; Franzini-Armstrong and Protasi, 1997; Sutko and Airey, 1997). In skeletal muscle, RyRs allow rapid release of Ca^{2+} from the sarcoplasmic reticulum (SR) during excitation-contraction (e-c) coupling. Electron microscopy shows that RyRs, called feet (Franzini-Armstrong, 1970), are organized in ordered arrays at specialized domains of the SR, called junctional SR (jSR). jSR feet are closely associated with regions of exterior membranes containing a second key molecule in e-c coupling, the dihydropyridine receptors (DHPRs) (Jorgensen et al., 1989; Flucher et al., 1990; Yuan et al., 1991). DHPRs are L-type Ca^{2+} channels, which act as voltage sensors in skeletal type e-c coupling (Rios and Brum, 1987; Tanabe et al., 1988; Adams et al., 1990; Beam et al., 1992). Their interaction with RyRs is responsible for transduction of exterior membrane depolarization into release of Ca^{2+} from the SR during e-c coupling (Fosset et al., 1983; Rios and Brum, 1987; Tanabe et al., 1988). The functional unit resulting from the association of jSR domains containing RyRs with exterior membrane domains containing DHPRs is called the calcium release unit (CRU).

Three RyR isoforms, exhibiting different pharmacological properties, have been isolated from a variety of tissues: RyR1, also known as the skeletal isoform (Takeshima et al., 1989; Zorzato et al., 1990); RyR2, or the cardiac isoform (Nakai et al., 1990; Otsu et al., 1990); and RyR3, or brain isoform (Hakamata et al., 1992; Chen et al., 1997). This terminology is based on the timing and tissue of initial purification, but further studies have shown that none of the three isoforms are entirely tissue-specific.

RyR1 and RyR3, or their nonmammalian equivalents α and β, are both present in some skeletal muscles (Airey et al., 1990; Olivares et al., 1991; Lai et al., 1992; Murayama and Ogawa, 1992; Giannini et al., 1995; Ledbetter et al., 1994; O'Brien et al., 1995; Conti et al., 1996). Skeletal muscles may contain either approximately equal amounts of RyR1 and RyR3 (muscles in amphibia, reptiles, birds, and most fish muscles), or RyR1 only (adult fast twitch mammalian muscle, some fish muscles), or predominantly RyR1 coexpressed with low levels of RyR3 (late embryonic and slow twitch mammalian muscles). For reviews see Sorrentino and Volpe (1993), Sorrentino (1995), Block et al.

(1996), Sutko and Airey (1997), and Franzini-Armstrong and Protasi (1997).

It is clear that RyR1 plays a more important role than RyR3 both in e-c coupling and in muscle differentiation. Muscles that express either very little or no RyR3 show normal e-c coupling, and some have extremely large and rapid Ca^{2+} transients upon stimulation (for example, the toadfish swim bladder muscle, which contains only RyR1; O'Brien et al., 1993; Rome et al., 1996). Although physiological studies in RyR3 knockout mice show some modest impairment of tension development during early postnatal muscle development, muscle differentiation and e-c coupling appear normal (Barone et al., 1998). On the other hand, no example of skeletal muscle lacking RyR1 expression is known to exist in nature, and muscles with null mutations of RyR1 all show total failure of e-c coupling and poor development. This is especially evident in the mouse, where RyR3 is not normally abundant (Takeshima et al., 1994; Buck et al., 1997), and in the chicken, where the β-isoform (equivalent to RyR3) is normally present with the α-isoform (equivalent to RyR1) in approximately equal amounts (Airey et al., 1990, 1993a; Ivanenko et al., 1995). In view of the above observations, it has been proposed that RyR3 may play a less direct role during e-c coupling, perhaps being secondarily activated after the opening of RyR1 (Rios et al., 1991).

It is important to know what role RyR3 may play in the structural organization of calcium release units. A direct opportunity to make such an inquiry is offered by 1B5 cells, a mouse skeletal line that carries a null mutation for RyR1. Differentiated 1B5 cells express several CRU proteins, but neither RyR1 nor RyR3 (Moore et al., 1998). The cells develop a SR system that makes junctions with the surface membrane and with primitive transverse (T) tubules, despite the lack of RyRs (Protasi et al., 1998). These junctions contain triadin and DHPRs, but of course lack RyRs or feet, and thus are dyspedic CRUs (dCRUs). These CRUs do not permit Ca^{2+} release in response to depolarization, caffeine, or 4-m-chloro-cresol (Moore et al., 1998; see also the accompanying report, Fessenden et al., 2000). Dyspedic CRUs in 1B5 cells resemble the great majority of dCRUs in the developing myotubes of RyR1-null mice, which develop in the absence of RyR1 and in the presence of very low levels of RyR3 (Takeshima et al., 1994; Takekura et al., 1995a; Takekura and Franzini-Armstrong, 1999). In CRUs of normal skeletal muscle cells, RyRs and DHPRs are arranged in highly ordered arrays with related parameters. RyRs are disposed in a tetragonal arrangement, and groups of four DHPRs, or tetrads, are associated with alternate RyRs, forming a related array (Franzini-Armstrong and Nunzi, 1983; Block et al., 1988; Franzini-Armstrong and Kish, 1995; Protasi et al., 1997). In 1B5 cells, despite the absence of RyRs, both DHPRs and triadin maintain their ability to form discrete groups located at dCRUs. However, DHPRs do not maintain the normal tetradic arrangement

(Protasi et al., 1998). Arrays of DHPR tetrads can be restored in differentiated 1B5 cells by transfection with RyR1 cDNA, indicating that the formation of tetrads requires anchoring of DHPRs on RyR1s (Protasi et al., 1998). In the present study we characterize in detail the effect of RyR1 expression on CRU structure, and, in addition, we define the effect of RyR3 expression. We find that both RyR1 and RyR3 are appropriately targeted to junctional sites, so that their cytoplasmic domains are located between the SR and exterior membrane, bridging the gap between the two. Both RyR1 and RyR3 are arranged in ordered arrays in the junctional SR in the absence of the other isoform. However, while expression of RyR1 restores the formation of DHPR tetrads in the surface membrane, expression of RyR3 does not, suggesting that RyR3 does not link to DHPRs at the junctions. Similar cultures transfected with RyR3, using the same helper free transduction system, have been shown by others to produce functional protein that undergoes spontaneous Ca^{2+} release, caffeine-induced Ca^{2+} release, but not depolarization-induced e-c coupling (Ward et al., 2000; Moore et al., 1999; see also the accompanying paper, Fessenden et al., 2000).

MATERIALS AND METHODS

Cell culturing

The methods used to create the 1B5 cell line are described in detail elsewhere (Moore et al., 1998). The cells were expanded at 37°C in low-glucose DME medium containing 20% fetal bovine serum, 100 units/ml penicillin, 100 μg/ml streptomycin, and additional 2 mM L-glutamine (growth medium). After ~48 h the cells were replated on thermanox coverslips (Nunc, Naperville, IL) covered with Matrigel (Collaborative Biomedical Products, Bedford, MA). When they reached ~70% confluence, growth medium was replaced with differentiation medium (containing 2% heat-inactivated horse serum instead of 20% of fetal bovine serum) to induce differentiation. The medium was changed every day, and the cells were fixed 5–6 days later.

cDNA packaging in HSV-1 virions and cell transfection

RyR1 and RyR3 cDNAs were packaged into HSV-1 amplicon virions, using the helper virus-free packaging system. The methods are described in detail elsewhere (Fraefel et al., 1996; Wang et al., 2000). Four to five days after differentiation had begun, the cells were infected with 1 ml of differentiation medium containing HSV1 virions at 4×10^5 infectious units/ml (a moiety of infection of ~3). This mixture was removed ~2 h later and replaced with 2 ml of differentiation medium. The cells were fixed ~24 h after infection.

Preparation of RyR3 site-directed antibody

A polyclonal antibody (RyR3-Ab) against a 13-amino acid region specific for RyR3 and containing a C-terminal cysteine (KKRRGQKVEKPEC) was prepared using standard procedures. One milligram of keyhole limpet hemocyanin-conjugated peptide was injected into a rabbit. The antisera were collected after 14 days post-injection of the third to fifth boost. RyR3

antibody was affinity purified using a peptide-agarose column prepared using Sulfo-Link gel (Pierce, Rockford, IL).

Immunoblotting the RyR3 antibody

Diaphragm and cardiac SR microsomes were denatured in sodium dodecyl sulfate (SDS) sample buffer (2% SDS, 2%, b-mercaptoethanol, 0.1 M Tris-HCl (pH 6.8), 10% glycerol) for 5 min at 95–100°C, separated on 3–12% SDS polyacrylamide gels, and transferred to Immobilon-P membranes at 4°C at 400 mA for 1–3 h followed by 1A for 14–16 h. Membranes were blocked for 1 h at room temperature with 5% nonfat dry milk and 0.1% Tween 20 in phosphate-buffered saline (PBS) and incubated for 3 h at room temperature with either RyR3-Ab or a monoclonal antibody specific for RyR1 (D110; Gao et al., 1997) in PBS containing 1% nonfat dry milk and 0.1% Tween 20. After washing, the bound antibody was detected with horseradish peroxidase-conjugated anti-rabbit or anti-mouse IgG, using 3,3-diaminobenzidine and H_2O_2. Fig. 1 shows immunoreactivity of the polyclonal antibody specific for RyR3 in diaphragm muscle (*lane 2*). The very minor amount of RyR3 in cardiac muscle cannot be detected using these loading conditions (*lane 1*). A specific anti-RyR1 antibody detected a band that runs slightly higher than RyR3 (*lane 3*).

Immunohistochemistry

The cells were fixed in methanol for a minimum of 20 min at $-20°C$, blocked in PBS containing 1% BSA and 10% goat serum for 1 h, and incubated first with primary antibodies and then with secondary antibodies (conjugated to cyanine 3 (CY3), Texas Red (TR), or fluorescein isothiocyanate (FITC); Jackson ImmunoResearch Laboratories, Lexington, KY), respectively, for 2 h and 1 h at room temperature. Code, specificity, working dilution, original reference, and the sources of primary antibodies are as follows: 34C, recognizes both RyR1 and RyR3, 1:10, Airey et al. (1990), Developmental Studies Hybridoma Bank (University of Iowa); no. 5, anti-RyR1, 1:200, Flucher et al. (1993), gift of Dr. S. Fleischer; RyR3-Ab, anti-RyR3, 1:100, characterized in this paper; 21A6, anti-α_1DHPR, 1:250, Morton and Froehner (1987), Chemicon International (Temecula, CA); GE4.90, anti-triadin, 1:500, Caswell et al. (1991), gift of Dr. A. H. Caswell. The specimens were viewed either in an inverted fluorescence microscope (Olympus IX70) or in a scanning confocal microscope (LSM510; Carl Zeiss, Switzerland).
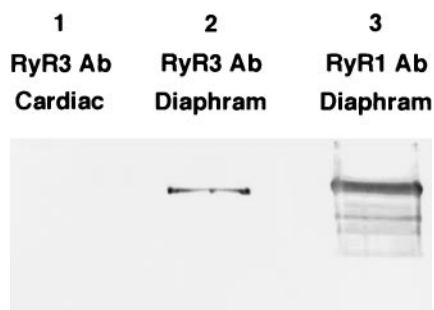

FIGURE 1   Immunoblots of cardiac and diaphragm microsomes. *Lane 1*: Cardiac microsomes and polyclonal RyR3 antibody. *Lanes 2* and *3*: Diaphragm microsomes, polyclonal RyR3 antibody, and monoclonal RyR1 D110 antibody. The polyclonal RyR3 antibody shows reactivity with diaphragm RyR3 (*lane 2*) but not with cardiac RyR2 (*lane 1*) or the slightly slower migrating RyR1 in the diaphragm (*lane 3*). The minor amount of RyR3 in cardiac muscle cannot be detected under these loading conditions (*lane 1*).

Electron microscopy

The cells were washed twice in PBS at 37°C, fixed in 3.5% glutaraldehyde in 0.1 M sodium cacodylate buffer (pH 7.2), and then kept in fixative for up to 1–4 weeks at 4°C before further use. For thin sectioning the cells were postfixed in 2% OsO_4 for 2 h at room temperature and then contrasted in saturated uranyl acetate either for 4 h at 60°C or overnight at room temperature. The samples were embedded in Epon 812, and the sections were stained in uranyl acetate and lead for ~8 min each.

For freeze fractures the glutaraldehyde-fixed cells were infiltrated with 30% glycerol. A small piece of the coverslip was mounted with the cells facing a droplet of 30% glycerol, 20% polyvinyl alcohol on a gold holder and then frozen in liquid nitrogen-cooled propane (Cohen and Pumplin, 1979; Osame et al., 1981). The coverslip was flipped off to produce a fracture that followed the culture surface originally facing the coverslip. The fractured surfaces were shadowed with platinum unidirectionally at 45° and then replicated with carbon in a freeze-fracture apparatus (model BFA 400; Balzers S.p.A., Milan, Italy). Sections and replicas were photographed in a 410 electron microscope (Philips Electron Optics, Mahwah, NJ).

Data and measurements

Data were obtained from the following databases. For control cells, the database from a previous study (Protasi et al., 1998) consisted of 13 freeze fractures from eight differentiated cultures and five embeddings from three cultures. In addition, one freeze fracture was performed on a nontransfected culture in the present study, and 16 coverslips (from 16 cultures) and 12 coverslips (from 12 cultures) were immunolabeled, respectively, with anti-α_1s-DHPR antibodies and anti-triadin. For RyR1 and RyR3 infections, 34 coverslips (from 21 cultures) and 20 coverslips (from 13 cultures) were immunolabeled, respectively, with anti-RyR antibodies. For RyR1 infections, six freeze-fracture runs were performed on dishes from five cultures, and four embeddings were made from four separate dishes in two different cultures. For RyR3, six freeze-fracture runs were performed on five dishes from five different cultures, and four embeddings were made using four dishes from four different cultures. The culture dishes used for electron microscopy (EM) were parallel to cultures that showed positive RyR labeling.

Quantitative data were obtained as follows:

1. The number of cells with various aspects of protein expression and/or arrangement (see Results) was estimated from counts of cells through direct view of immunolabeled specimens in the epifluorescence microscope (see Table 1).

2. The width of the junctional gap was measured in images of dCRUs and CRUs, in which both the SR and surface membranes were clearly delineated, indicating an appropriate orientation of the membranes perpendicular to the plane of sectioning. Junctions fitting these criteria were selected from a series of micrographs depicting all junctions that could be seen in various sections, until a total reached 20 junctions in each category. Three to four lines were drawn randomly across the junction, and measurements were taken at the position of these lines.

3. The spacings between feet were measured in junctions showing several (three to nine) evenly spaced feet within the junctional gap. The average distance was calculated by dividing the distance between the most widely separated feet by the number of feet in the group minus one. All available junctions, up to a total of 30, were measured.

4. The spacing between DHPR tetrads in RyR1 transduced cells were measured in micrographs from groups of tetrads that were selected for being most complete. The location of incomplete tetrads was estimated by the dotting approach (see Protasi et al., 1997).

5. The method for estimating frequency of tetrads is explained in the Results.

Preparation of figures

Pictures and negatives were scanned using a Color Flatbed Scanner UMAX Power Look II at 300 dpi. Figures were mounted using Adobe Photoshop, v. 4.01, and labeled using Canvas, v. 3.5.4 (Deneba Software).

RESULTS

Formation of RyR-containing CRUs in RyR1- and RyR3-infected cells

1B5 cells were immunolabeled with antibodies against two proteins of the junctional SR, RyR and triadin, and one protein of the surface membrane/T tubule, the α_1s subunit of the DHPR.

Differentiating 1B5 cells fuse into large multinucleated myotubes. Five days after the withdrawal of growth factors, most of the multinucleated myotubes and some of the remaining unfused cells express α_1s-DHPR and triadin (Fig. 2, *A* and *B*). The two proteins are clustered in intensely fluorescent small foci located at, or very close to, the cell surface (see Protasi et al., 1998). 1B5 cells do not express any detectable amount of either RyR1 or RyR3 (Moore et al., 1998) and are negative for labeling by an anti-RyR antibody that recognizes both isoforms (Figs. 2 *C* and 3 *B*). We have previously defined a relationship between the formation of large multinucleated myotubes, the presence of dCRUs (dyspedic peripheral couplings, dyads, and triads), and the presence of DHPRs and triadin foci (Protasi et al., 1998). 1B5 cells that fuse into myotubes form dCRUs, structures that are specific to muscle fibers, and express triadin and DHPRs, two skeletal muscle-specific proteins. These cells are clearly differentiated, according to the classic definition of differentiation. 1B5 cells have defective myofibrils and dyspedic CRUs that lack feet (Protasi et al., 1998). In these two respects 1B5 cells resemble the in vivo differentiated myofibers found in RyR1-null embryos (Takekura et al., 1995a).

Infection of 1B5 cells with HSV-1 amplicon virions containing a cDNA encoding either RyR1 or RyR3 gave excellent results, in both transduction efficiency and protein expression. In addition, HSV-1 amplicon virions did not cause any cell death and did not affect either general structural parameter, such as cell size and shape, or the level of differentiation (see below). Up to 60–70% of the myotubes examined 24 h after infection reacted positively with anti-RyR antibodies in both RyR1- and RyR3-infected cultures (Figs. 3, *C* and *D*). This is in agreement with data obtained independently from comparable viral titers (presented in the accompanying paper; Fessenden et al., 2000). The presence of RyR expression in the cells did not appear to change the expression of DHPR and triadin and their formation of foci (Figs. 3 *A* and 5). Nondifferentiated cells act as negative controls for the DHPR and triadin antibodies, and differentiated cells that do not express RyRs act as negative controls for the RyR antibodies. Examples of the latter are shown in Figs. 2 *C* and 3 *B*. A negative control for the secondary antibody is also shown in figure 2 *D* of Protasi et al. (1998).

Microscopic examination of multinucleated myotubes at high optical resolution revealed that transduction with either RyR1 or RyR3 produced similar small, intense RyR foci, which form a punctate pattern at the periphery of the cell, either at the surface or in its vicinity (Fig. 4, *A* and *C*). The interior of cells exhibiting foci is practically devoid of any RyR antibody labeling, as clearly shown in images through the center (Fig. 4 *B*). Double labeling for RyR and either DHPR or triadin demonstrates colocalization of foci of the latter two junctional proteins with foci of either RyR1 or RyR3. Fig. 5 illustrates cells transduced with RyR1 (Fig. 5, *A–D*) and RyR3 (Fig. 5, *E–H*) and double labeled for RyR (shown in *red*) and either DHPR or triadin (shown in *green*). The DHPR/triadin-positive foci also containing RyR appear as yellow spots (Fig. 5, *B, D, F,* and *G*). Cells that have only green foci (either DHPR or triadin) and no evidence of RyR presence (Fig. 5, *A, C,* and *E*) are identical to cells in control
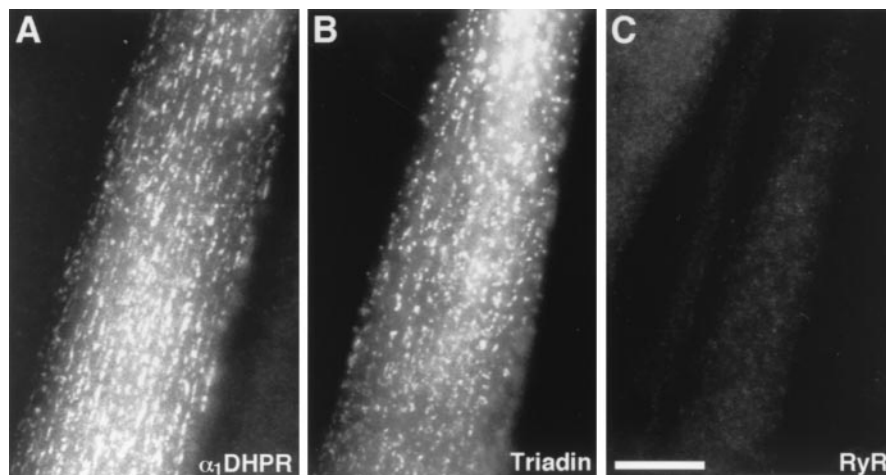

FIGURE 2 Expression and localization of DHPR and triadin in differentiated 1B5 cells. (*A* and *B*) Immunolabeling of 1B5 cells 5 days after differentiation with antibodies against α_1-DHPR and triadin shows that most of the large myotubes contain frequent, discrete foci of the two proteins at or near the cell surface. Undifferentiated cells do not express either DHPR or triadin (not shown). (*C*) An antibody that recognizes both RyR1 and RyR3 (34C) shows an absence of both isoforms (fluorescence microscope Olympus IX70). Bar, 25 μm.
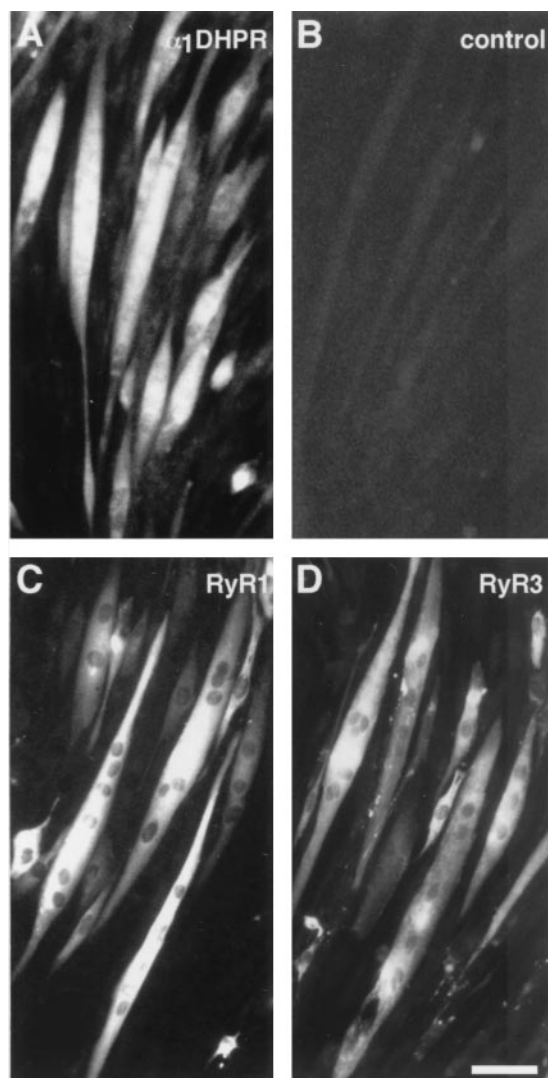
FIGURE 3 DHPR and RyR expression in RyR-transduced 1B5 cells. Five days after differentiation, 1B5 myotubes in RyR-transduced cultures express α_1-DHPR (*A*) and either RyR1 (*C*) or RyR3 (*D*). (*B*) Control cells stained with anti-RyR antibodies demonstrate lack of expression before exposure to HSV-1 virions. Protein distribution and colocalization of DHPRs and RyRs are shown in Figs. 4 and 5. Statistical analysis is given in Table 1. Anti-RyR antibody used: 34C (fluorescence microscope Olympus IX70). Bar, 200 μm.

cultures (see Protasi et al., 1998), and thus they obviously are not transduced. Cells that express triadin, DHPRs, and the induced RyR are both differentiated and transduced.

In thin-section electron microscopy, differentiated 1B5 cells are identified by the presence of peripherally located SR-exterior membrane junctions that lack feet (dCRUs), as previously described (see Protasi et al., 1998). The dCRUs are typically found in the larger cells, and they are either in the form of peripheral couplings or of dyads/triads involving wide and short surface membrane invaginations (probably representing primitive T-tubules). A correlation between the presence of dCRUs and that of foci of triadin and

DHPRs has previously been established (Protasi et al., 1998). Partially developed myofibrils are often but not always present, and endoplasmic reticulum (ER) networks in the cell interior are very scarce in differentiated 1B5 cells. In thin sections of transduced cultures, differentiated cells also contain numerous peripherally located dCRUs, but scarce internal SR, and often some myofibrils, resembling the differentiated cells in control cultures. The novel feature introduced by the RyR transduction is the appearance of feet in the SR-surface junctions of some cells. The feet are clustered within CRUs, and in most cases the spacing between them is quite regular, indicating the formation of ordered arrays in both RyR1- and RyR3-transduced cells (Fig. 6, *arrows*). The spacing between feet is 31 $\pm$ 3 nm in RyR3-infected cells and 36 $\pm$ 6 nm in RyR1-infected cells (mean $\pm$ 1 SD from 30 junctions each). For each junction the measured spacing is the average of the spacing between three to nine adjacent feet. The data were obtained from embeddings of four dishes (four independent infected cultures) in the case of RyR3 and from embeddings of four dishes (two independent infected cultures) in the case of RyR1. The spacing in RyR1-expressing cells is greater and more variable than in RyR3-expressing cells, probably because of the interesting fact that most of the RyR1 junctions have smaller clusters of feet and thus the measurements are less accurate.

Clusters of feet of both isoforms are found within CRUs that are located at or very near the surface membrane and are almost never seen in the center core of the cell. This is in perfect agreement with the location of RyR/DHPR/triadin foci detected by immunolabeling (Figs. 4 and 5). In addition, there is a bimodal distribution of CRUs, i.e., all CRUs in a given cell either are dyspedic (dCRUs; Fig. 5, *D* and *H*) or contain feet (RyR$^+$ CRUs; Fig. 5, *A–C* and *E–G*). This also correlates well with the immunofluorescence observations showing that after infection with RyR virion differentiated cells have either no RyR foci or abundant RyR foci throughout. Two to three cells (among the several hundred observed in this set of experiments) presented an internal set of SR cisternae, the surfaces of which were studded with an extensive array of feet (not shown) of the type previously described in RyR1-transfected Chinese hamster ovary cells (Takekura et al., 1995b).

RyR$^+$ and dCRUs in different cells from the same cultures differ in the width of the gap separating the SR and exterior membranes. The dyspedic junctional gap is narrower and more variable in width than the RyR$^+$ gap, in agreement with previous observations on dyspedic and normal junctions of mouse muscle in vivo (Takekura et al., 1995a) and with the narrow gap of control 1B5 cells (Protasi et al., 1998). The difference is quite obvious to the eye (Fig. 6; compare dyspedic junctions to RyR$^+$ junctions). The gap width was measured in junctions from RyR1- and RyR3-infected cells that were either RyR$^+$ or dyspedic. The measured widths were 12.4 $\pm$ 2.0 for the RyR3 and 12.2 $\pm$ 1.9

FIGURE 4 RyR1 and RyR3 distribution in transduced, differentiated myotubes. (*A* and *C*) Both RyR isoforms are clustered within intensely labeled foci. Images through the center (*B*) and at the bottom surface (*C*) of the same cell show that the foci are located at or very close to the cell surface. Punctate labeling for RyR is present in large myotubes and in some smaller, spindle-shaped cells that are also multinucleated. Anti-RyR antibody used: 34C (fluorescence microscope Olympus IX70). Bar, 25 μm.
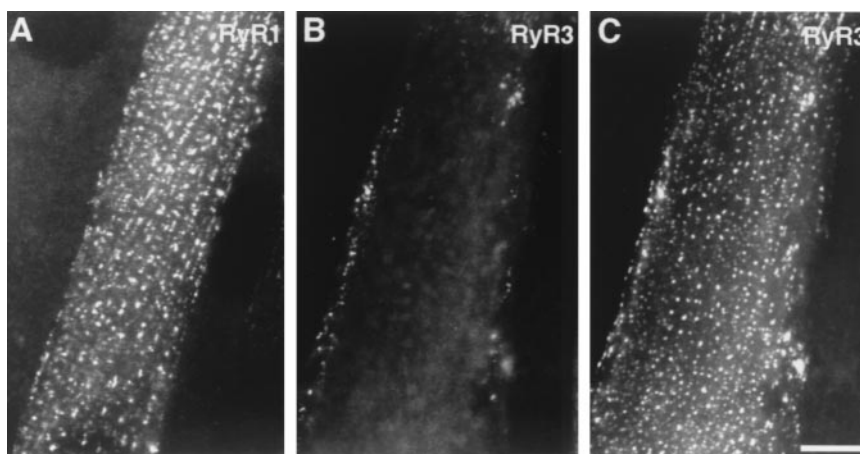
for the RyR1-containing junctions and 9.1 $\pm$ 3.6 nm and 9.3 $\pm$ 3.1 for the dyspedic junctions in the same embeddings (mean $\pm$ 1 SD, from 20 junctions, two to four measurements at each junction). The width of the combined RyR$^+$ junctions is significantly different from that of the combined dyspedic junctions (Student's *t*-test, $p < 0.0001$), but the widths of junctions containing RyR1 and RyR3 do not differ.

Interestingly, a variation in the en bloc staining procedure for EM resulted in a junctional gap width that is not different in dyspedic and RyR$^+$ CRUs. In the different procedure, RyR1- and RyR3-infected 1B5 cells had been exposed to uranyl acetate in 70% EtOH rather than the laboratory's standard procedure involving aqueous solution. The widths of the junctional gaps for control, RyR1$^+$, and RyR3$^+$ junctions in these cells are approximately equal to each other: 11.4 $\pm$ 2.1, 11.4 $\pm$ 2.1 and 11.5 $\pm$ 1.2 nm (from 20, 27, and 14 junctions; 80, 135, and 70 measurements). The significance of this is considered at the end of the Discussion.

It is known that RyR-containing CRUs can form in dysgenic muscle cells lacking α_1s-DHPR, and thus it is not surprising that few cells (less than 1%) in cultures transduced with either type of RyR have red foci with no evidence for the presence of DHPRs (not shown). These cells are transduced, and the RyRs are located in peripherally placed foci that contain very little or no DHPR (not shown). While the colocalization with triadin was ubiquitous in cells transduced with RyR1 (Fig. 5 *D*), some cultures transduced with RyR3 showed few cells (again less than 1%) with RyR3$^+$ foci, and either no or an undetectable level of triadin (Fig. 5 *H*). Note, however, that in most cells expressing RyRs in the absence of DHPR/triadin foci the RyR remain located within the internal reticular ER network.

Transduced undifferentiated cells

Numerous mononucleated cells and a few of the larger multinucleated myotubes in the cultures infected with either RyR isoform contain an extensive reticular network pervading the entire cell, presumably the endoplasmic reticulum, which is intensely labeled by the antibody (Fig. 7 *A*). Coexistence of the internal-reticular and the peripheral-punctate patterns of RyR labeling is very rare (Fig. 7 *B*). In double immuno labeling the cells with an intense RyR internal labeling and no peripheral RyR foci lack DHPR and/or triadin foci (Fig. 5 *E*), suggesting that these cells are not differentiated. The presence of the internal intensely RyR$^+$ network correlates well with the presence of numerous extended rough ER cisternae in EM images from cells of infected cultures (compare Fig. 7, *A* and *C*). The ER cisternae form part of a network pervading the whole cell and containing a granular material (Fig. 7 *D*). Such extended rough ER (rER) cisternae, forming complex networks, are never present in noninfected cells, which have fewer and much smaller isolated rER profiles (see figure 4 *A* in Protasi et al., 1998). In agreement with immunolabeling, the cells containing the extended ER network are usually smaller and lack evidence of differentiation (CRUs and myofibrils). We note that obvious arrays of feet are not visible on the surface of the extensive ER network in these cells, but the presence of a few randomly distributed individual feet cannot be excluded. Considering the excellent quantitative correlation between morphology in the present study (Fig. 7 *A*) and functional recovery presented in the accompanying paper (Fessenden et al., 2000), it is likely that cells possessing a reticular pattern of RyR distribution are the same cells that fail to have e-c coupling but recover responses to caffeine. On the basis of the functional data and of the lack of CRUs, the cells are classified as transduced undifferentiated. They are not considered further in this study.

Quantitation of immunolabeled cultures

Clustering of DHPRs and the formation of ordered DHPR arrays are detected by freeze fracture, and two points about this method need to be considered. First, this technique samples $\sim$3-mm circles, which are small portions of the coverslip on which cells are cultured. Second, the position-
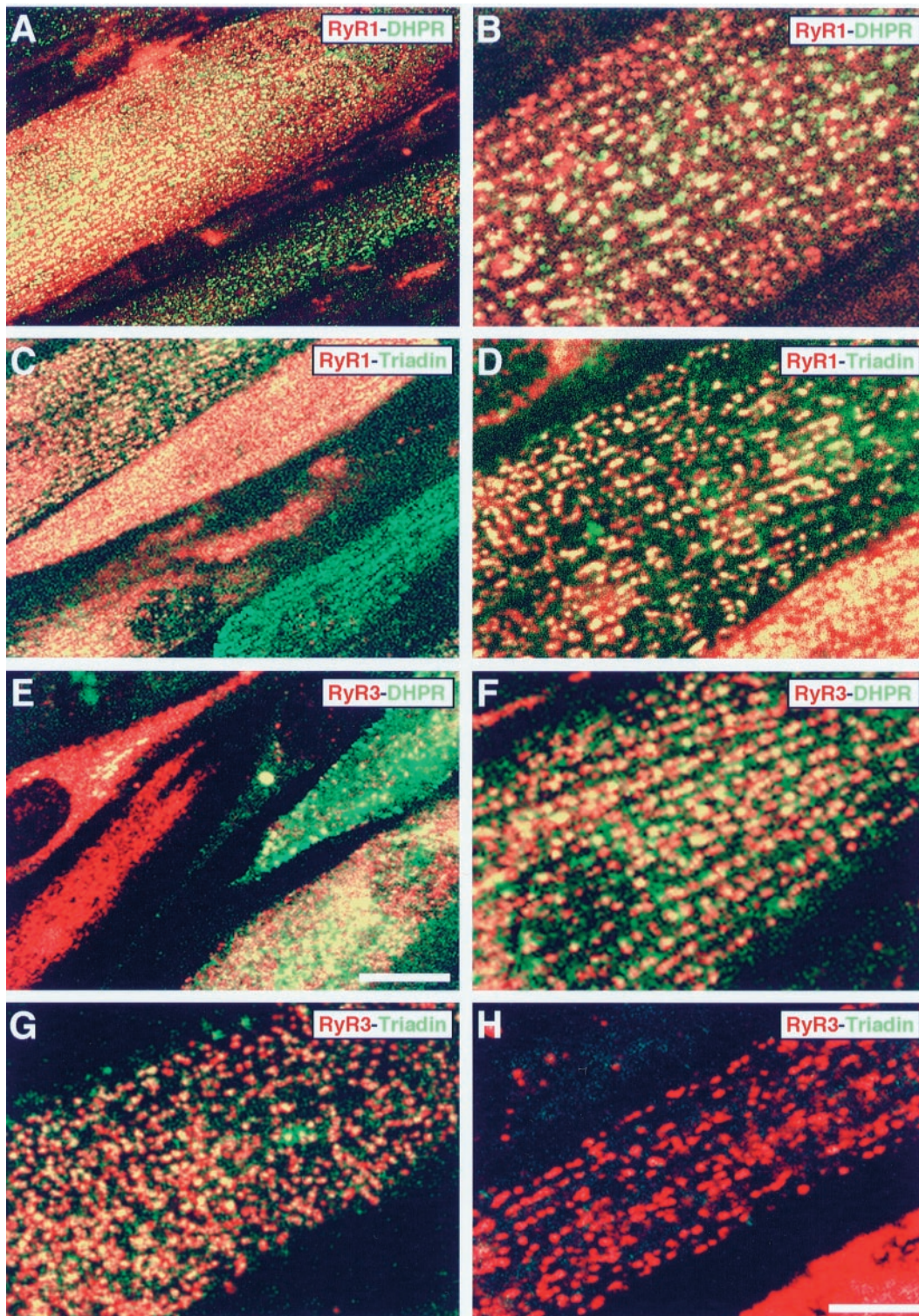
FIGURE 5   Immunolabeling for RyR1/RyR3 (shown in *red*) and either DHPR or triadin (shown in *green*). Yellow indicates colocalization of RyR and DHPR/triadin. (*A* and *C*) Cells with yellow peripheral foci contain both RyR1 and DHPR (or triadin). These cells are transduced and differentiated. Green cells contain only DHPR (or triadin) but no RyR; these cells are differentiated, but not transduced. (*B* and *D*) RyR1 colocalize with either DHPR or triadin at peripherally located foci. Cells expressing a high level of RyR1 but little or no DHPR/triadin are not shown. (*E*) RyR3-transduced cells expressing either RyR3 (*red cells*) or DHPR (*green cells*) or both proteins (*yellow cells*). (*F* and *G*) Colocalization of RyR3 with either DHPR or triadin is obvious in these transduced and differentiated cells. (*H*) A rare cell that has peripheral foci containing RyR3 but not triadin, showing that RyR may be appropriately targeted to CRUs in the absence of triadin. Anti-RyR1 antibody used: no. 5; anti-RyR3 antibody used: RyR3-Ab (LSM510 confocal microscope; Carl Zeiss). Bars: *A, C,* and *E*, 50 μm; *B, D, F, G,* and *H*, 25 μm.
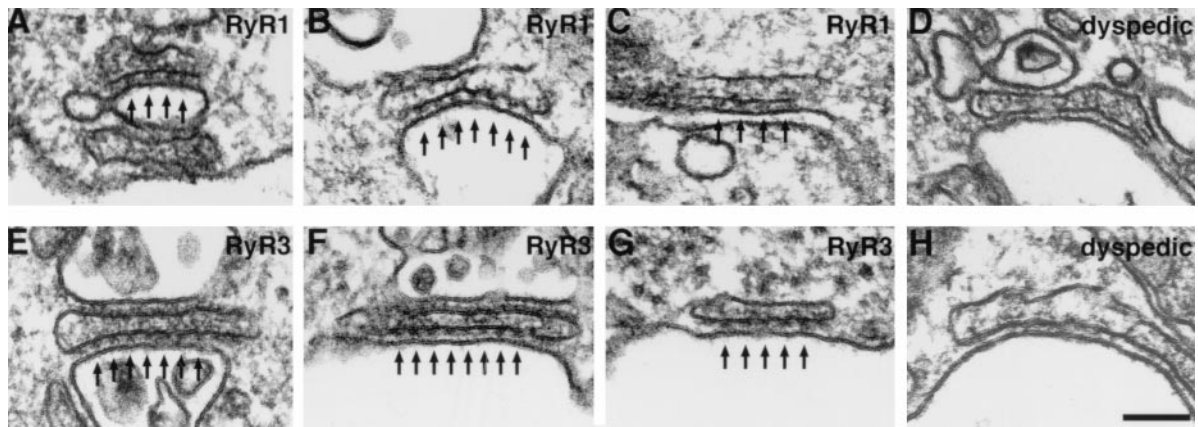
FIGURE 6 RyR1 and RyR3 are equally capable of forming arrays of feet. In RyR1- and RyR3-infected dishes, differentiated cells fall into two categories. Some cells have peripherally located CRUs that contain ordered arrays of feet (*arrows*; *A–C*, RyR1; *E–G*, RyR3). Other cells (*D* and *H*) exclusively have junctions with no feet (dyspedic). These two types of cells correspond to the transduced-differentiated and differentiated categories in Table 1. In these images the width of the junctional gap is wider in junctions containing feet than in dyspedic ones (compare *A–C* and *E–G* with *D* and *H*), but under different preparative procedures the width may be the same (see Results and Discussion). Bar, 0.1 µm.

ing of DHPR within clusters is the same in control and RyR3-infected 1B5 cells (see below). For these two reasons, it is very important to know that a sufficiently large number of differentiated-transduced cells are present within small areas of the coverslip. We obtained quantitative data on the frequency of various types of cells in infected cultures, using coverslips grown and treated in parallel with those used for freeze fracture. Coverslips from a culture dish were cut in half, and the two halves were stained either for DHPR or for RyR. Other coverslips from the same culture were
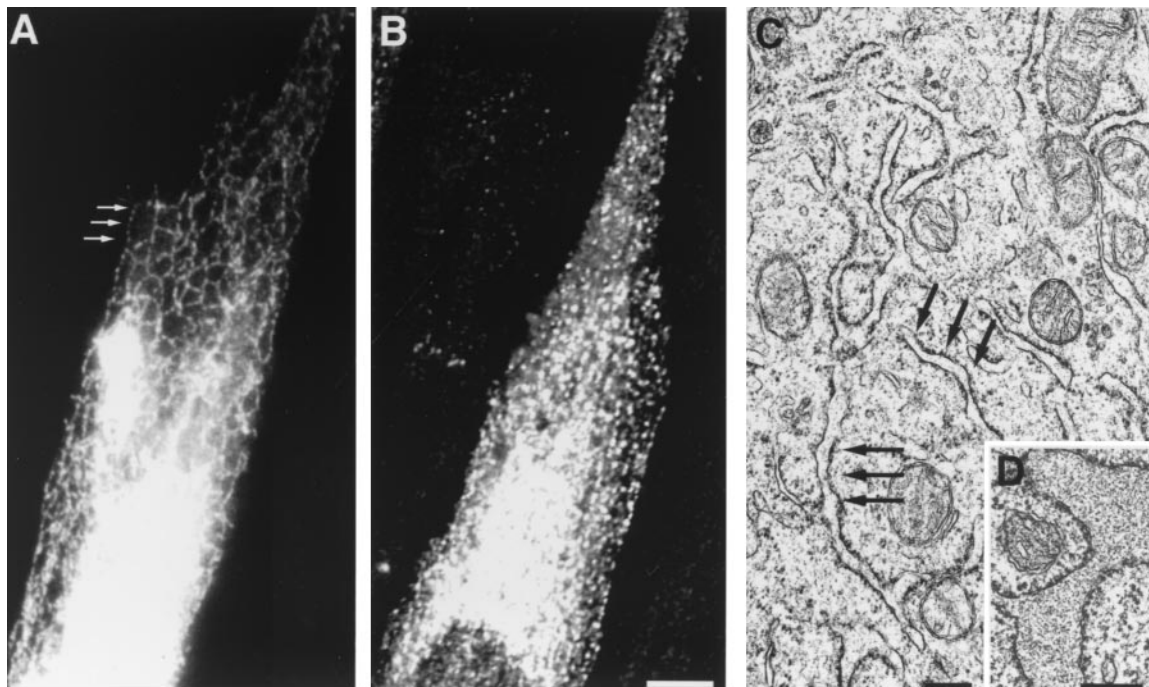

FIGURE 7 RyR1 and RyR3 remain in the endoplasmic reticulum of undifferentiated cells. (*A*) Several small cells expressing RyR1 and RyR3 show an extensive, reticular network in the cytoplasm, which labels with antibodies against RyR (*arrows*). (*B*) In very few cells the internal reticular and peripheral punctate RyR labeling coexist. We correlate the cells presenting the reticular network in the cytoplasm (such as the one in *A*) with cells containing an extensive rough ER (rER) network pervading the whole cytoplasm and filled with a grainy material (*C* and *D, arrows*). Cells with the extended internal rER do not have CRUs at their periphery (not differentiated) and are present only in infected cultures. Anti-RyR antibody used: 34C (LSM510 confocal microscope; Carl Zeiss). Bars: *A* and *B*, 25 µm; *C* and *D*, 0.25 µm.

TABLE 1 Frequency of cells positive for DHPR/triadin and for RyR, and of cells with a punctate RyR pattern

1 Culture	2 Antibody	3 Fields of view counted	4 No. of cells with DHPR/triadin in foci (differentiated)	5 No. of cells expressing RyR (total transduced)	6 No. of cells with punctate RyR foci (transduced-differentiated)	7 Ratio of differentiated to transduced-differentiated	8 Ratio of transduced-differentiated to total transduced
RyR1 1a	Anti-DHPR	53[*]	144 (2.7)			1.2	0.49
RyR1 1a	Anti-RyR	53[*]		240	117 (2.2)		
RyR1 1b	Anti-DHPR	53[*]	195 (3.7)			1.5	0.47
RyR1 1b	Anti-RyR	53[*]		276	130 (2.5)		
RyR1 2	Anti-DHPR	25[†]	165 (6.6)			4.4	0.43
RyR1 2	Anti-RyR	25[†]		86	37 (1.5)		
RyR3 1	Anti-DHPR	57[*]	159 (2.8)			1.7	0.28
RyR3 1	Anti-RyR	53[*]		300	85 (1.6)		
RyR3 2	Anti-triadin	22[†]	101 (4.6)			1.2	0.70
RyR3 2	Anti-RyR	22[†]		128	90 (4.1)		

[*]Indicates counts taken with 40× objective.

[†]Indicates counts taken with 63× objective.

In parentheses, the number of cells per field of view.

fixed for freeze fracture and thin sectioning. The number of cells per field of view that had labeled foci were counted in coverslips from five randomly chosen and well-differentiated cultures of cells transduced with virions containing either RyR1 or RyR3. The data are given in Table 1. Column 4 gives the counts of cells with peripheral foci of DHPR/triadin, which represent the number of differentiated cells. Column 5 gives the total number of cells that express RyR1 or RyR3. These numbers include cells with peripheral punctate and internal reticular patterns of RyR distribution. Column 6 gives the count of cells with a punctate pattern of peripheral RyR foci. These cells are both differentiated and transduced. The ratio between the number of differentiated and transduced-differentiated cells is given in column 7, and column 8 gives the ratio between transduced-differentiated cells and total number of transduced cells. In four experiments, approximately two out of three differentiated cells are also transduced. This means that in two out of three cells that show clusters of DHPRs in the freeze-fracture replica of the DHPR clusters are located in correspondence or RyR[+] CRUs. One RyR1 experiment was less successful (RyR1 no. 2), but even here, one out of four cells was transduced. The EM grid covers an area that is approximately nine times larger than the field of view of the 40× objective, and thus a significant number of cells that are differentiated and transduced should be present in each EM sample. Taken together with the data of Moore et al. (1998), these results reveal that these multinucleated myotubes forming RyR1 foci are capable of sustaining e-c coupling.

## DHPR arrangement in CRUs of cells expressing RyR1 and RyR3

Numerous previous publications have demonstrated that DHPRs are present in the surface membrane as large particles located within uniquely identifiable clusters that are easily visible in freeze-fracture replicas (Block et al., 1988; Takekura et al., 1994; Protasi et al., 1997, 1998).

Distribution of DHPRs in RyR1-transduced cultures will be described in detail first, because this helps in understanding results from RyR3-transduced cells. Clusters of DHPRs in RyR1-transduced cells are located within well-delimited patches of membrane (Fig. 8 *A*), which mostly exclude other, smaller intramembranous particles. All clusters of DHPRs contain some recognizable tetrads, defined as groups of four equal particles (each representing one DHPR) located at the corners of small squares (see details in Fig. 8). Other groups of DHPRs within the clusters are recognizable as incomplete tetrads that contain three particles occupying three corners of a square (see detail in *lower right corner* of Fig. 8 *A*). The centers of complete and incomplete tetrads mark an orthogonal pattern with a spacing of 41.2 ± 8.5 nm (mean $\pm$ 1 SD from 25 clusters of tetrads). Extending the pattern through the whole group of particles shows that all particles within the groups of DHPRs are located in close proximity to a tetrad center (Fig. 8 *B*). Along the diagonals of the tetragonal arrangement the average spacing is 58 nm (Fig. 8 *B, arrows*), which corresponds to twice the center-to-center distance between two adjacent feet. This ordered arrangement is identical to that found in normal skeletal muscles as well as in a muscle cell line (Block et al., 1988; Franzini-Armstrong and Kish, 1995; Protasi et al., 1997). A prominent feature of DHPR arrays in cells infected with RyR1 is the alignment of particles along two orthogonal directions that arises from the stereotyped positioning of individual DHPRs relative to the underlying subunits of RyRs (see Discussion and Block et al., 1988; Franzini-Armstrong and Kish, 1995).

We find three correlations between the distribution of tetrad arrays in freeze-fracture replicas and that of immunolabeled foci of RyRs. One is a 1:1 correspondence between cultures that show RyR foci and those that show

FIGURE 8 Infection with RyR1, but not RyR3, induces DHPR tetrad restoration in differentiated 1B5 cells. (*A*) In RyR1-transduced cells DHPR particles are grouped into tetrad arrays. Two tetrads are outlined by squares; these are shown at a higher magnification (*A, lower corners*). Some of the tetrads are incomplete; that is, one (or more) of the four elements is missing. A set of four complete tetrads is shown at on right side of *B*. (*B*) Dotting the center of each tetrad in the array of *A* results in an ordered orthogonal arrangement of dots. The spacing between the dots marking the center of tetrads in the direction of the arrows is twice the distance between feet, indicating that the normal skeletal 2:1 ratio between feet and tetrads is restored in these CRUs. (*C–G*) In RyR3-transduced and control cells, even if DHPR particles are clustered within junctional domains, they do not form tetrads. Bars, 0.1 μm.
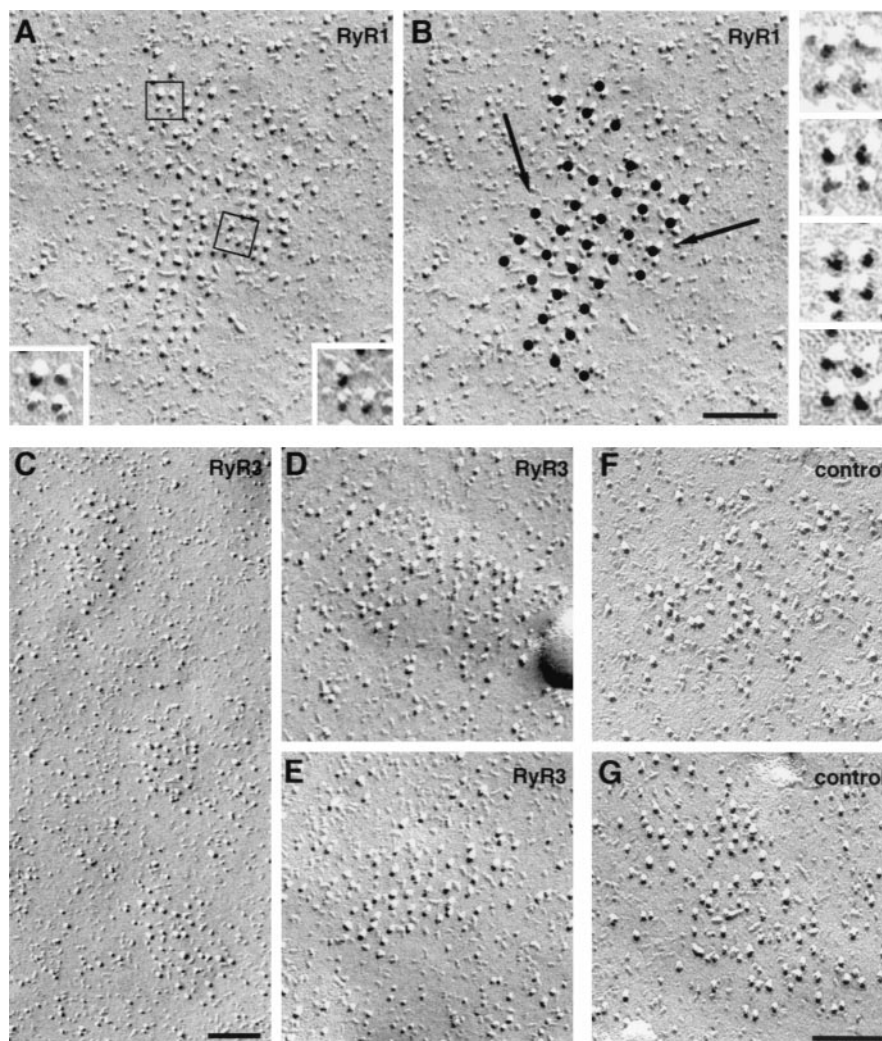
clusters of tetrads in fractures from parallel dishes. The second correlation is in the frequency of cells that have either structure. Replicas from culture dishes parallel to those used for RyR1 1a and b immunolabeling (see Table 1) show many (14–16 per EM grid) cells with surface clusters of DHPRs disposed in arrays of tetrads, some of them quite extensive (Fig. 8 *A*). On the other hand, a culture dish parallel to the RyR1 no. 2 experiment in Table 1, which had a lower number of transduced cells with RyR foci, showed fewer (two or three per EM grid) cells with tetrads after freeze fracture. The third correlation is in the distribution of tetrad arrays and foci in individual cells. Both freeze fracture and immunolabeling show a bimodal distribution in the sense that individual cells have either a large number of tetrad clusters per focus or none. These three correlations indicate that the presence of RyR1 foci has a predictive value for the presence of arrays of DHPR tetrads. This, of course, is also demonstrated by the colocalization of the two proteins shown by double immunolabeling (Fig. 5, *A* and *B*).

Fractures of RyR3-transduced cultures contain numerous myotubes with clusters of DHPRs, but no tetrads are seen in these junctions. In addition, there is no preferred linear alignment of the DHPR particles along orthogonal directions, indicating that the position of the majority of particles is not correlated to that of feet subunits. The clusters of DHPRs in cultures containing RyR3-transduced cells (Fig. 8, *C–E*) and in control cultures (Fig. 8, *F* and *G*) are not structurally different, except for a slightly domed shape of the membrane in some images from the transduced cells. The similarity between DHPR clusters of control and RyR3-transduced cultures raises the questions of whether the DHPR clusters detected by freeze fracture belong to cells that have been transduced with RyR3 and whether they correspond to foci of DHPRs that are colocalized with RyRs. The first part of the question is answered by the observation that cells with peripherally located RyR3 clusters constitute a considerable portion of the cells exposed to RyR3-containing virions. The ratio of differentiated cells (containing DHPR foci) and transduced-differentiated cells

(containing RyR) is ~3:2 (Table 1, column 7). The second part of the question is answered by the observation that either all or many of the DHPR foci are colocalized with RyR foci in the majority of the cells that were demonstrated to have foci of both proteins (Fig. 5 *F*). In our freeze-fracture replicas the entire cell surface facing the coverslip is visible and has been examined. Thus it is unlikely that co-localized DHPR and RyR3 clusters have been missed in this study.

Testing the random disposition of DHPRs in RyR3-expressing cells

Despite the fact that the disposition of DHPRs appears random in RyR3-transduced cells, it is possible that a small percentage of DHPRs are specifically linked to feet, thus acquiring a specific location relative to the feet arrays. To test for this possibility, the disposition of particles was assessed in DHPR clusters of RyR3-expressing cells versus those in control, and RyR1-expressing cells. Control cells provide parameters for a randomly generated arrangement of particles, while RyR1 cells provide parameters for tetrad arrays derived by steric linking of RyRs to feet subunits.

First we determined the frequency of tetrads in clusters from the three types of cells. We examined in detail 27 clusters of particles containing a total of 1170 particles (for control cells), 973 particles (for RyR3), and 716 particles (for RyR1). In the arrays from RyR1-transduced cells, 83% of the particles on average are part of complete tetrads or of tetrads containing three of the four DHPRs. The remaining particles are also part of tetrads, as indicated by their appropriate position in the array, but the tetrads in this case are reduced to two elements or one element. Note that most of the tetrads have a precise arrangement of particles (see details in Fig. 8), even if some are distorted during fracturing. In clusters from RyR3-infected cells and from control cells an average of 19% and 6% particles, respectively, is in groups that resemble tetrads, and in most of the groups of four particles the square disposition is highly distorted.

Second we determined whether a significant number of particles are aligned at spacing and along directions indicative of a possible interaction with feet subunits. Three parameters were measured for this analysis. Parameter A was the number of particles that are arranged in short linear arrays of three or more particles. In control cells, the percentage of particles that are aligned in groups of three to five is 28 ± 8 of the total (mean $\pm$ 1 SD, from a total of 1534 particles, in 24 clusters from four freeze fractures). In RyR3- and RyR1-expressing cells, the percentages are 15 ± 10 and 84 ± 24, respectively (from 3149 particles, 50 clusters, and five freeze fractures for RyR3; and 719 particles, 24 clusters, and one freeze fracture for RyR1). The differences between the means for RyR1 and RyR3 versus control are both significant ($p < 0.0001$), but the absolute values of the differences are in opposite directions, i.e.,

clusters in RyR3 cells have fewer aligned particles than the randomly disposed control clusters, while clusters in RyR1 cells have considerably more aligned particles than controls. We purposely made the sample of RyR3 cells selected larger than the others, to compensate for the fact that some of the clusters examined may belong to cells not expressing the ryanodine receptor.

Parameter B was the angle between lines tangent to the linear arrays of particles. In control and RyR3 cells the smaller of the two complementary angles at each line intersection was measured. The angles range from 0° to 90°, and the mean values between $45° \pm 25°$ and $49° \pm 24°$ (mean $\pm$ 1 SD, $n = 141$ and 166 angles). In RyR1 cells, the angles between lines tangent to the sides of two or three adjacent tetrads were measured. The angle sizes are tightly clustered between 80° and 90°, with a mean of $85° \pm 5°$ ($n = 70$ angles). The differences between the means of control and RyR3 versus RyR1 are significant (Student's *t*-test, $p < 0.0001$), but the control and RyR3 means are not significantly different ($p = 0.071$).

Parameter C was the percentage of aligned groups of particles in which the spacing between the particles corresponds to that of particles associated with feet subunits. The assessment was made by tracing the positions of particles in adjacent tetrads of RyR1-expressing cells on a transparent sheet and superimposing it on the aligned groups. The percentage of aligned groups of particles with a spacing equal to that found in tetrad arrays is $15 \pm 17\%$ (from a total of 24 groups) for the control and $19 \pm 24\%$ (from 40 groups) in RyR3 cells. The difference between the two means is not statistically significant (Student's *t*-test, $p = 0.389$).

The conclusion from the two types of analysis is that the arrangement of DHPR particles in RyR3-transduced cells is not significantly different from that of control cells, but differs considerably from that in cells that express RyR1.

DISCUSSION

Naturally occurring and engineered null mutations of RyR1 and RyR3 have provided initial information on the contribution of RyR to the formation, structure, and function of CRUs. Both in vivo and in vitro studies of specimens lacking either one or both RyR isoforms clearly show that 1) the formation of CRUs, in the form of SR/exterior membrane junctions, and 2) the proper targeting of junctional proteins to CRUs do not require RyRs (Takeshima et al., 1994; Takekura et al., 1995a; Airey et al., 1993a,b; Protasi et al., 1998; Barone et al., 1998). Because RyR3 is expressed relatively late in the differentiation process of both murine (Bertocchini et al., 1997) and avian (Airey et al., 1993a,b) muscles, it cannot be required either for initial junction formation or for appropriate targeting of RyR1 to the junctional sites. In this work we show that all of the RyR1 expressed within the SR of differentiated 1B5 cells is

incorporated at peripherally located junctions. Thus, RyR1 is appropriately and efficiently targeted to CRUs in the absence of RyR3. On the other hand, published evidence regarding the behavior of RyR3 in the absence of RyR1 is limited. CRUs containing electron-dense material resembling feet (presumably RyR3) are only 1–2% of the total number of CRUs in the RyR1-null mouse (Takekura et al., 1995a; Takeshima et al., 1995) and crooked neck dwarf chicken muscles (T. Watanabe, C. Franzini-Armstrong, and J. L. Sutko, unpublished observations). In these two systems it is not clear whether the scarcity of such junctions is due to low expression of the protein or to poor targeting of RyR3 in the absence of RyR1, possibly due to muscle dysgenesis.

Efficient expression of RyR3 in our system allows us to show that this isoform can be as effectively targeted to CRUs as RyR1 is, even in the absence of the latter. This makes preferential targeting of RyR3 in dyspedic muscle cells to sites other than CRUs unlikely. In addition, our data show that RyR3, like RyR1, can independently form ordered arrays within CRUs.

Once RyRs are located in CRUs, they are in the appropriate position for interactions with DHPRs, which in 1B5 cells are represented by the skeletal muscle-specific α_1s isoform. Differences in the disposition of α_1s-DHPR in RyR1- and RyR3-containing CRUs have profound functional implications for this interaction. The presence of RyR1 imposes the grouping of DHPRs into tetrads, positioning of tetrads in tetragonal arrays, and consequent alignment of DHPRs along orthogonal lines. This specific positioning of DHPRs is characteristic of skeletal muscle calcium release units and implies a precise relationship between individual DHPRs and RyR1 subunits, indicative of a stereospecific link between the two proteins. The putative site of DHPR-RyR interaction has been hypothesized to be located between two of the domains that form the clamp region at the corners of the RyR tetramer (Samso et al., 1999). This would position the four DHPRs off center relative to the RyR subunits, in agreement with previous structural observations (Franzini-Armstrong and Kish, 1995; Protasi et al., 1997).

The colocalization of α_1s-DHPR and RyR3 in double-labeling experiments implies proximity between these two molecules in RyR3-expressing 1B5 cells. However, our analysis shows that the disposition of α_1s-DHPRs in RyR3 cells lacks the grouping into tetrads and the alignment along orthogonal directions that is indicative of a link to RyR subunits. Therefore the relative positions of α_1s-DHPR and RyR3 are similar to that of α_1c-DHPR and RyR2 in cardiac muscle (Sun et al., 1995; Protasi et al., 1996). In both cases the molecules are in close proximity to each other at the junctions, but they are not linked in a stereospecific manner. Despite this structural similarity, skeletal muscle fibers and 1B5 cells that express only RyR3 differ from cardiac muscle in that e-c coupling fails, even in the presence of extracel-

lular Ca^{2+} (Takeshima et al., 1994; Ivanenko et al., 1995). The data in the accompanying paper (Fessenden et al., 2000) and from Ward et al. (2000) clearly show that the failure of e-c coupling in 1B5 myotubes expressing RyR3 is not due to a dysfunction of the expressed RyR3. The failure is also not attributable to differences in the functional properties of RyR2 and RyR3, because both isoforms have a high sensitivity to Ca^{2+} (see Franzini-Armstrong and Protasi, 1997, for a review) and thus are candidates for calcium-induced calcium release. Instead, the probable explanation lies in the properties of the DHPRs. α_1s-DHPR has slow activation kinetics and its Ca^{2+} currents are almost negligible, particularly when it is not linked to RyR1

On the basis of the above observations, we present models of the relative dispositions of RyRs and DHPRs in junctions containing either one or both RyR isoforms. In all images RyRs are shown in ordered arrays with previously established parameters (Ferguson et al., 1984). RyR1 are pale blue, RyR3 are green, and DHPRs are shown as black circles. The overall disposition of feet has been shown to be similar in muscles that contain either no RyR3 or variable amounts of it (compare Franzini-Armstrong, 1973; Ferguson et al., 1984; Block et al., 1988). Thus, we assume that the positioning of feet in the arrays is independent of the contributions of various isoforms. Minor variations cannot be excluded, however. In the presence of only RyR1, which is the case in our RyR1-expressing cells as well as several muscle types, DHPRs are grouped in tetrads (Fig. 9 A). The four DHPRs within the tetrads (represented by *four black circles*) have the same position relative to the four subunits of the RyRs, and the tetrads are associated with alternating feet (see Block et al., 1988). In the presence of RyR3 only (Fig. 9 B), DHPRs are randomly grouped at the junctions. Thus, DHPRs are located in exterior membrane domains that face feet arrays, but, as in cardiac muscle (Sun et al., 1995; Protasi et al., 1996), they do not have a stereospecific position relative to the feet arrays.

In muscles that express both RyR isoforms in approximately equal stoichiometries, three arrangements of the two isoforms are possible, and each predicts a specific positioning of DHPRs. One possibility is that RyR3 is precisely alternated with RyR1 (Fig. 9 C). In this case tetrads would be located on alternating feet, just as in Fig. 9 A. The second possibility, based on the self-assembly property of RyR3 observed in the present study, is that RyR1 and RyR3 group in a stochastic fashion, resulting in variable clustering of the two types of channels (Fig. 9 D). In this case, tetrads would be less frequent than in Fig. 9, A and C, and the large areas devoid of tetrads would have no DHPRs (as depicted in Fig. 9 D), or, what is more likely, they would be occupied by randomly arranged DHPRs. The third possibility (not shown) is that the two RyRs are clustered in separate but neighboring CRUs. Data from the literature (Airey et al., 1990; Flucher et al., 1999) show that both RyR1 and RyR3 (or their nonmammalian equivalents) are located at triads
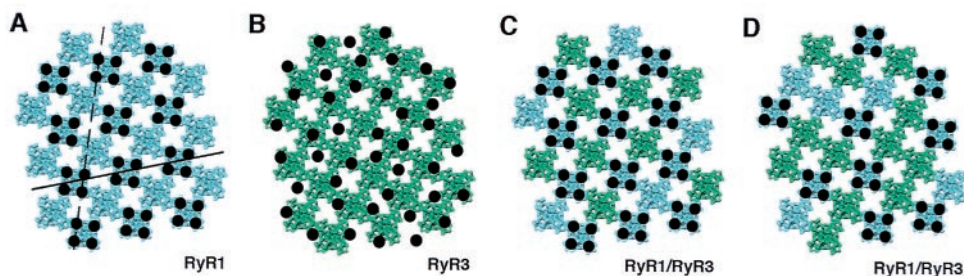
FIGURE 9 (*A* and *B*) Diagrams modeling the relative positions of DHPRs and RyRs in peripheral couplings of 1B5 cells transduced with either RyR1 or RyR3. The arrays of feet are constructed by combining the guidelines given in Franzini-Armstrong and Kish (1995) with the detailed outline of the ryanodine receptor reconstructed by Radermacher et al. (1994). RyR1 is shown in pale blue and RyR3 in green; DHPRs are shown as black circles. (*A*) DHPRs are in a fixed position relative to the four subunits of the feet forming tetrads that associate with alternating feet. Both tetrads and feet are rotated by 8° clockwise relative to the line connecting the centers of adjacent feet and tetrads (*solid line* in *A*). This rotation results in a visible alignment of DHPRs along orthogonal directions (*dashed line* in *A*). The skew angle and alignment of DHPRs have been fully described in the literature (Block et al., 1988; Franzini and Kish, 1995; Protasi et al., 1997) and are restored in 1B5 cells expressing RyR1. (*B*) The disposition of DHPRs in RyR3-transduced cells is random, and the distance between DHPRs and feet subunits is variable, although never very large. (*C* and *D*) Two hypothetical dispositions in CRUs of muscle fibers containing mixtures of RyR1 and RyR3. These two models illustrate two possible arrangements of RyRs and tetrads in muscles where both RyR isoforms (1 and 3) are present in approximately equal stoichiometry. Note that the model predicts a lower density of tetrads in *D* than in *C*. It is also possible that the two isoforms are segregated in adjacent but separate junctions (not shown).

but do not exclude this situation. The result of a separation of RyRs in different CRUs would be that CRUs containing tetrads and others with randomly disposed DHPRs would be present in the same muscle. At the moment the precise disposition of DHPRs in muscles with well-established high contents of both RyR isoforms is not known, but it is clear that once that disposition is known it will be possible to choose between the three possibilities.

RyR3's failure to restore either DHPR tetrads or a linear arrangement of DHPRs along orthogonal directions demonstrates that a specific link between RyR3 and α_1s-DHPR is either absent or quite rare. The latter observation suggests a possible difference in the activation mechanism of RyR1 and RyR3. The accompanying paper (Fessenden et al., 2000) indeed demonstrates that RyR3 in the absence of RyR1 is not capable of responding to depolarization of myotubes induced by either electrical or chemical means. It is thus expected that RyR3 activation is secondary to RyR1 activation during e-c coupling.

The junctional gap separating the SR from surface membranes in dCRUs has been reported to be significantly smaller than the feet-occupied gap of normal junctions (Takekura et al., 1995a), and we have confirmed this finding (Protasi et al., 1998; present work). The narrow width of the dyspedic gap implies that the putative docking protein responsible for holding SR and exterior membranes in close proximity to each other is shorter than the feet, and it would have to stretch out, break, or disappear when the feet occupy the gap. However, we have also found that in a different preparative procedure, the width of the dyspedic gap is equal to the normal gap. Because shrinkage is a frequent artifact in EM specimen preparation, particularly when little protein is present, we suggest that the wider gap is probably closer to reality, and the narrower gap of dyspedic junctions

does not have a functional meaning. However, the narrow gap is useful in helping to define which junctions lack feet. We further suggest that the docking protein, when identified, will have to be sufficiently large to cross a 10–12-nm gap but does not have to stretch or disappear when feet occupy the junction.

REFERENCES

Adams, B. A., T. Tanabe, A. Mikami, S. Numa, and K. G. Beam. 1990. Intramembrane charge movement restored in dysgenic skeletal muscle by injection of dihydropyridine receptor cDNAs. *Nature.* 346:569–572.

Airey, J. A., M. D. Baring, C. F. Beck, Y. Chelliah, T. J. Deerinck, M. H. Ellisman, L. J. Houenou, D. D. McKemy, J. L. Sutko, and J. Talvenheimo. 1993a. Failure to make normal alpha ryanodine receptor is an early event associated with the crooked neck dwarf (cn) mutation in chicken. *Dev. Dyn.* 197:169–188.

Airey, J. A., C. F. Beck, K. Murakami, S. J. Tanksley, T. J. Deerinck, M. Ellisman, and J. L. Sutko. 1990. Identification and localization of two triad junction foot protein isoforms in mature avian fast twitch skeletal muscle. *J. Biol. Chem.* 265:14187–14194.

Airey, J. A., T. J. Deerinck, M. H. Ellisman, L. J. Houenou, A. Ivanenko, J. L. Kenyon, D. D. McKemy, and J. L. Sutko. 1993b. Crooked neck

dwarf (cn) mutant chicken skeletal muscle cells in low density primary cultures fail to express normal alpha ryanodine receptor and exhibit a partial mutant phenotype. *Dev. Dyn.* 197:189–202.

Barone, V., F. Bertocchini, R. Bottinelli, F. Protasi, P. D. Allen, C. Franzini-Armstrong, C. Reggiani, and V. Sorrentino. 1998. Contractile impairment and structural alterations of skeletal muscles from knockout mice lacking type 1 and type 3 ryanodine receptors. *FEBS Lett.* 422: 160–164.

Beam, K. G., B. A. Adams, T. Niidome, S. Numa, and T. Tanabe. 1992. Function of a truncated dihydropyridine receptor as both voltage sensor and calcium channel. *Nature.* 360:169–171.

Bertocchini, F., C. Ovitt, A. Conti, V. Barone, H. Schoeler, R. Bottinelli, C. Reggiani, and V. Sorrentino. 1997. Requirement for the ryanodine receptor type 3 isoform Ca^{2+} release channel for efficient contraction in neonatal muscles. *EMBO J.* 16:6956–6963.

Block, B. A., T. Imagawa, K. P. Campbell, and C. Franzini-Armstrong. 1988. Structural evidence for direct interaction between the molecular components of the transverse tubule/sarcoplasmic reticulum junction in skeletal muscle. *J. Cell Biol.* 107:2587–2600.

Block, B. A., J. O'Brien, and J. Franck. 1996. The role of ryanodine receptor isoforms in the structure and function of the vertebrate triad. *Soc. Gen. Physiol. Ser.* 51:47–65.

Buck, E. D., A. H. Nguyen, I. N. Pessah, and P. D. Allen. 1997. Dyspedic mouse skeletal muscle expresses major elements of the triadic junction but lacks ryanodine receptor protein and function. *J. Biol. Chem.* 272: 7360–7367.

Caswell, A. H., N. R. Brandt, J. P. Brunschwig, and S. Purkerson. 1991. Localization and partial characterization of the oligomeric disulfide-linked molecular weight 95,000 protein (triadin) which binds the ryanodine and dihydropyridine receptors in skeletal muscle triadic vesicles. *Biochemistry.* 30:7507–7513.

Chen, S. R. W., X. Li, K. Ebisawa, and L. Zhang. 1997. Functional characterization of the recombinant type 3 Ca^{2+} release channel (ryanodine receptor) expressed in HEK293 cells. *J. Biol. Chem.* 272: 24234–24246.

Cohen, S. A., and D. W. Pumplin. 1979. Clusters of intramembranous particles associated with binding sites for alpha-bungarotoxin in cultured chick myotubes. *J. Cell Biol.* 82:494–516.

Conti, A., L. Gorza, and V. Sorrentino. 1996. Differential distribution of ryanodine receptor type 3 (RyR3) gene product in mammalian skeletal muscles. *Biochem. J.* 316:19–23.

Coronado, R., J. Morrissette, M. Sukhareva, and D. M. Vaughan. 1994. Structure and function of ryanodine receptors. *Am. J. Physiol.* 266: C1485–C1491.

Fessenden, J. D., Y. Wang, R. A. Moore, S. R. W. Chen, P. D. Allen, and I. N. Pessah. 2000. Divergent physiological and pharmacological properties of ryanodine receptor type 1 and 3 expressed in a myogenic cell line. *Biophys. J.* 79:000–000.

Ferguson, D. G., H. Schwartz, and C. Franzini-Armstrong. 1984. Subunit structure of junctional feet in triads of skeletal muscle. A freeze-drying, rotary-shadowing study. *J. Cell Biol.* 99:1735–1742.

Flucher, B. E., S. B. Andrews, S. Fleisher, A. R. Marks, A. H. Caswell, and J. A. Powell. 1993. Triad formation: organization and function of the sarcoplasmic reticulum calcium release channel and triadin in normal and dysgenic muscle in vitro. *J. Cell Biol.* 123:1161–1174.

Flucher, B. E., A. Conti, H. Takeshima, and V. Sorrentino. 1999. Type 3 and type 1 ryanodine receptors are localized in triads of the same mammalian skeletal muscle fiber. *J. Cell Biol.* 146:621–629.

Flucher, B. E., M. E. Morton, S. C. Froehner, and M. P. Daniels. 1990. Localization of the α_1 and α_2 subunits of the dihydropyridine receptor and ankyrin in skeletal muscle triads. *Neuron.* 5:339–351.

Fosset, M., E. Jaimovich, E. Delpont, and M. Lazdunski. 1983. [³H]Nitrendipine receptors in skeletal muscle. *J. Biol. Chem.* 258:6086–6092.

Fraefel, C., S. Song, F. Lim, P. Lang, L. Yu, Y. Wang, P. Wild, and A. I. Geller. 1996. Helper virus-free transfer of HSV-1 plasmid vectors into neuronal cells. *J. Virol.* 70:7190–7197.

Franzini-Armstrong, C. 1970. Studies of the triad. *J. Cell Biol.* 47: 488–499.

Franzini-Armstrong, C. 1973. Studies of the triad: IV. Structure of the junction in frog slow fibers. *J. Cell Biol.* 56:120–128.

Franzini-Armstrong, C., and J. W. Kish. 1995. Alternate disposition of tetrads in peripheral couplings of skeletal muscle. *J. Muscle Res. Cell Motil.* 16:319–324.

Franzini-Armstrong, C., and G. Nunzi. 1983. Junctional feet and particles in the triads of a fast-twitch muscle fibre. *J. Muscle Res. Cell Motil.* 4:233–252.

Franzini-Armstrong, C., and F. Protasi. 1997. The ryanodine receptor of striated muscles, a complex capable of multiple interactions. *Physiol. Rev.* 77:699–729.

Gao, L., A. Tripathy, X. Lu, and G. Meissner. 1997. Evidence for a role of C-terminal amino acid residues in skeletal muscle Ca^{2+} release channel (ryanodine receptor) function. *FEBS Lett.* 412:223–226.

Giannini, G., A. Conti, S. Mammarella, M. Scrobogna, and V. Sorrentino. 1995. The ryanodine receptor/calcium channel genes are widely and differentially expressed in murine brain and peripheral tissues. *J. Cell Biol.* 128:893–904.

Hakamata, Y., J. Nakai, H. Takeshima, and K. Imoto. 1992. Primary structure and distribution of a novel ryanodine receptor/calcium release channel from rabbit brain. *FEBS Lett.* 312:229–235.

Ivanenko, A., D. D. McKemy, J. L. Kenyon, J. A. Airey, and J. L. Sutko. 1995. Embryonic chicken skeletal muscle cells fail to develop normal excitation-contraction coupling in the absence of the alpha ryanodine receptor. Implications for a two-ryanodine receptor system. *J. Biol. Chem.* 270:4220–4223.

Jorgensen, A. O., A. C-Y. Shen, W. Arnold, A. T. Leung, and K. P. Campbell. 1989. Subcellular distribution of the 1,4-dihydropyridine receptor in rabbit skeletal muscle in situ: an immunofluorescence and immunocolloidal gold-labeling study. *J. Cell Biol.* 109:135–147.

Lai, F. A., Q. Y. Liu, L. Xu, A. El-Hashem, N. R. Kramarcy, R. Sealock, and G. Meissner. 1992. Amphibian ryanodine receptor isoforms are related to those of mammalian skeletal or cardiac muscle. *Am. J. Physiol.* 263:C365–C372.

Ledbetter, M. W., J. K. Preiner, C. F. Louis, and J. R. Mickelson. 1994. Tissue distribution of ryanodine receptor isoforms and alleles determined by reverse transcription polymerase chain reaction. *J. Biol. Chem.* 269:31544–31555.

Meissner, G. 1994. Ryanodine receptor/Ca^{2+} release channels and their regulation by endogenous effectors. *Annu. Rev. Physiol.* 56:485–508.

Moore, R. A., J. D. Fessenden, Y. Wang, S. R. W. Chen, P. D. Allen, and I. N. Pessah. 1999. Viral expression of RyR1 and RyR3 in a myogenic cell line lacking native RyR. *Biophys. J.* A394.

Moore, R. A., H. Nguyen, J. Galceran, I. N. Pessah, and P. D. Allen. 1998. A transgenic myogenic cell line lacking ryanodine receptor protein for homologous expression studies: reconstitution of Ry_1R protein and function. *J. Cell Biol.* 140:843–851.

Morton, M. E., and S. C. Froehner. 1987. Monoclonal antibody identifies a 200 kDa subunit of the dihydropyridine-sensitive calcium channel. *J. Cell Biol.* 262:11904–11907.

Murayama, T., and Y. Ogawa. 1992. Purification and characterization of two ryanodine-binding protein isoforms from sarcoplasmic reticulum of bullfrog skeletal muscle. *J. Biochem.* 112:514–522.

Nakai, J., T. Imagawa, Y. Hakamata, M. Shigekawa, H. Takeshima, and S. Numa. 1990. Primary structure and functional expression from cDNA of the cardiac ryanodine receptor/calcium release channel. *FEBS Lett.* 271:16917.7.

O'Brien, J., G. Meissner, and B. A. Block. 1993. The fastest contracting muscles of nonmammalian vertebrates express only one isoform of the ryanodine receptor. *Biophys. J.* 65:2418–2427.

O'Brien, J., H. H. Valdivia, and B. A. Block. 1995. Physiological differences between the alpha and beta ryanodine receptors of fish skeletal muscle. *Biophys. J.* 68:471–482.

Olivares, E. B., S. J. Tanksley, J. A. Airey, C. F. Beck, Y. Ouyang, T. J. Deerinck, M. H. Ellisman, and J. L. Sutko. 1991. Nonmammalian vertebrate skeletal muscles express two triad junctional foot protein isoforms. *Biophys. J.* 59:1153–1163.

Osame, M., A. G. Engel, C. J. Rebouche, and R. E. Scott. 1981. Freeze-fracture electron microscopic analysis of plasma membranes of cultured muscle cells in Duchenne dystrophy. *Neurology.* 31:972–979.

Otsu, K., H. F. Willard, V. K. Khanna, F. Zorzato, N. M. Green, and D. H. MacLennan. 1990. Molecular cloning of cDNA encoding the Ca^{2+} release channel (ryanodine receptor) of rabbit cardiac muscle sarcoplasmic reticulum. *J. Biol. Chem.* 265.

Protasi, F., C. Franzini-Armstrong, and P. D. Allen. 1998. Role of the ryanodine receptors in the assembly of calcium release units in skeletal muscle. *J. Cell Biol.* 140:831–842.

Protasi, F., C. Franzini-Armstrong, and B. E. Flucher. 1997. Coordinated incorporation of skeletal muscle dihydropyridine receptors and ryanodine receptors in peripheral couplings of BC_3H1 cells. *J. Cell Biol.* 137:859–870.

Protasi, F., H.-H. Sun, and C. Franzini-Armstrong. 1996. Formation and maturation of calcium release units in developing and adult avian myocardium. *Dev. Biol.* 173:265–278.

Radermacher, M., V. Rao, R. Grassucci, J. Frank, A. P. Timerman, S. Fleisher, and T. Wagenknecht. 1994. Cryo-electron microscopy and three-dimensional reconstruction of the calcium release channel/ryanodine receptor from skeletal muscle. *J. Cell Biol.* 127:411–423.

Rios, E., and G. Brum. 1987. Involvement of dihydropyridine receptors in excitation-contraction coupling in skeletal muscle. *Nature.* 325:717–720.

Rios, E., J. Ma, and A. Gonzales. 1991. The mechanical hypothesis of excitation-contraction coupling in skeletal muscle. *J. Muscle Res. Cell Motil.* 12:127–129.

Rome, L. C., D. A. Syme, S. Hollingworth, S. L. Lindstedt, and S. M. Baylor. 1996. The whistle and the rattle: the design of sound producing muscles. *Proc. Natl. Acad. Sci. USA.* 93:8095–8100.

Samso, M., R. Trujillo, G. B. Gurrola, H. H. Valdivia, and T. Wagenknecht. 1999. Localization of imperatoxin A binding sites on the skeletal muscle ryanodine receptor by cryo-electron microscopy. *Biophys. J.* 76:A301.

Sorrentino, V. 1995. The ryanodine receptor family of intracellular calcium release channels. *Adv. Pharmacol.* 33:67–90.

Sorrentino, V., and P. Volpe. 1993. Ryanodine receptors: how many, where and why? *Trends Pharmacol. Sci.* 14:98–105.

Sun, X.-H., F. Protasi, M. Takahashi, H. Takeshima, D. G. Ferguson, and C. Franzini-Armstrong. 1995. Molecular architecture of membranes involved in excitation–contraction coupling of cardiac muscle. *J. Cell Biol.* 129:659–673.

Sutko, J. L., and J. A. Airey. 1997. Ryanodine receptor Ca^{2+} release channel: does diversity in form equal diversity in function? *Phys. Rev.* 76:1027–1071.

Takekura, H., L. Bennett, T. Tanabe, K. G. Beam, and C. Franzini-Armstrong. 1994. Restoration of junctional tetrads in dysgenic myotubes by dihydropyridine receptor cDNA. *Biophys. J.* 67:793–804.

Takekura, H., and C. Franzini-Armstrong. 1999. Correct targeting of dihydropyridine receptors and triadin in dyspedic mouse skeletal muscle in vivo. *Dev. Dyn.* 214:372–380.

Takekura, H., M. Nishi, T. Noda, H. Takeshima, and C. Franzini-Armstrong. 1995a. Abnormal junctions between surface membrane and sarcoplasmic reticulum in skeletal muscle with a mutation targeted to the ryanodine receptor. *Proc. Natl. Acad. Sci. USA.* 92:3381–3385.

Takekura, H., H. Takeshima, S. Nishimura, M. Takahashi, T. Tanabe, V. Flockerzi, F. Hoffman, and C. Franzini-Armstrong. 1995b. Co-expression in CHO cells of two muscle proteins involved in e-c coupling. *J. Muscle Res. Cell Motil.* 16:465–480.

Takeshima, H., M. Iino, H. Takekura, M. Nishi, J. Kuno, O. Minowa, H. Takano, and T. Noda. 1994. Excitation-contraction uncoupling and muscular degeneration in mice lacking functional skeletal muscle ryanodine-receptor gene. *Nature.* 369:556–559.

Takeshima, H., S. Nishimura, T. Matsumoto, H. Ishida, K. Kangawa, N. Minamino, H. Matsuo, M. Ueda, M. Hanaoka, and T. Hirose. 1989. Primary structure and expression from complementary DNA of skeletal muscle ryanodine receptor. *Nature.* 339:439–445.

Takeshima, H., T. Yamazawa, T. Ikemoto, H. Takekura, M. Nishi, T. Noda, and M. Iino. 1995. Ca^{2+} induced Ca^{2+}-release in myocytes from dyspedic mice lacking the type-1 ryanodine receptor. *EMBO J.* 14: 2999–3006.

Tanabe, T., K. G. Beam, J. A. Powell, and S. Numa. 1988. Restoration of excitation-contraction coupling and slow calcium current in dysgenic muscle by dihydropyridine receptor complementary DNA. *Nature.* 336: 134–139.

Wang, Y., C. Fraefel, F. Protasi, R. A. Moore, J. D. Fessenden, I. N. Pessah, A. DiFrancesco, X. Breakefield, and P. D. Allen. 2000. HSV-1 amplicon vectors are a highly efficient gene delivery system for skeletal muscle myoblasts and myotubes. *Am. J. Physiol. Cell.* 47:C619–C623.

Ward, C. W., M. F. Schneider, D. Castillo, F. Protasi, Y. Wang, S. R. W. Chen, and P. D. Allen. 2000. Expression of ryanodine receptor 3 produces Ca^{2+} sparks in dyspedic myotubes. *J. Physiol. (Lond.).* 525: 91–103.

Yuan, S., W. Arnold, and A. O. Jorgensen. 1991. Biogenesis of transverse tubules and triads: immunolocalization of the 1,4-dihydropyridine receptor, TS28, and the ryanodine receptor in rabbit skeletal muscle developing in situ. *J. Cell Biol.* 112:289–301.

Zorzato, F., J. Fujii, K. Otsu, M. Phillips, N. M. Green, F. A. Lai, G. Meissner, and D. H. MacLennan. 1990. Molecular cloning of cDNA encoding human and rabbit forms of the Ca^{2+} release channel (ryanodine receptor) of skeletal muscle sarcoplasmic reticulum. *J. Biol. Chem.* 265:2244–2256.